

DEPOLARIZED UPWARD AND DOWNWARD MULTIPLE SCATTERING FROM A VERY ROUGH SURFACE

C.-Y. Hsieh

Electrical and Computer Engineering Department
National Kaohsiung Marine University
Kaohsiung, Taiwan

A. K. Fung

Electrical Engineering Department
University of Texas
Arlington, Texas, USA

Abstract—From a very roughly random surface the backscattering enhancement is predicted due to the constructive interference of multiple surfaces scattering. For specialized surfaces involving roughness large compared with the incident wavelength, the backscattering enhancement takes place. The phenomenon of backscatter enhancement becomes evident for both larger normalized surface height and surface rms slope. In this paper we take further study to predict the backscattering enhancement mainly comes from upward multiple scattering. On the contrary the downward multiple scattering has no contributions to the scatter strength of backscattering enhancement. The model developed in this paper is based upon the integral equation method and able to predict this phenomenon of multiple scattering and backscattering enhancement. The depolarized multiple scattering makes much contribution along the plane of incidence from random rough surfaces, but depolarized single scattering makes little contributions. The total multiple scattering strength is the summation of upward and downward multiple scattering strength. In comparison of model prediction of total multiple scattering strength with measured data along the specular plane, excellent agreement is obtained.

1 Introduction

2 Model Development

2.1 Scattered Power and Coefficients

2.2 Shadowing Functions

2.3 Scattering Coefficients with Shadowing Functions

3 Shadowing Functions

3.1 Shadowing Functions under the Integral Sign

4 Model Prediction

4.1 Contribution Comparisons of Single and Multiple Scattering

4.2 Upward and Downward Multiple Scattering

5 Comparisons with Measurements

Appendix A.

References

1. INTRODUCTION

The experimental study of backscattering enhancement from characterized random surfaces was studied by L. Ailes-Sengers in 1995 [1]. The comparisons of Monte Carlo numerical studies and experimental measurement of backscattering enhancement from 2-D perfectly conducting random rough surfaces was made in 1996 [2, 3]. Up to date a theoretical model for studying the backscattering enhancement and the relationship among the backscattering enhancement and the multiple scattering is still lacking. Further the study of upward or downward multiple scattering making major contributions to backscattering enhancement is also lacking.

In this paper we develop the scattering model to predict the multiple scattering and backscattering enhancement and the relationship among them. Due that the phase terms of Green's function and its derivative in the integral equation pairs is a possible candidate for the backscattering enhancement from very rough surfaces, the model developed in this paper is based upon the integral equation pairs with tangential electric and magnetic surface fields.

First the governing equations for the tangential surface fields on a dielectric surface can be written as the sum of the standard Kirchhoff and complementary surface fields (Figure 1). The estimates the tangential electric and magnetic fields at a surface point can be obtained by the tangential surface fields. After estimating the

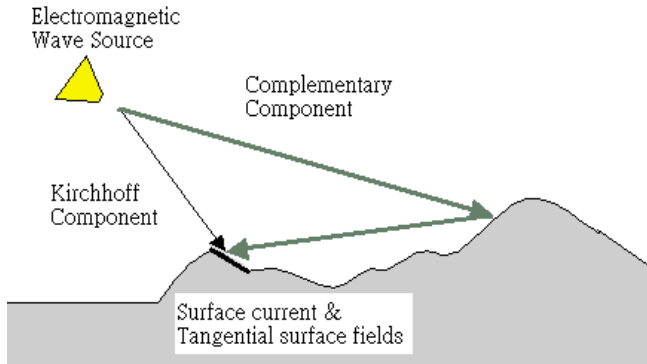


Figure 1. Tangential surface current induced by Kirchhoff and complementary scattering.

tangential surface fields the scattered field can be found in terms of them. With the scattered field expression the average scattered power and scattered coefficient can be found subsequently, the scattering coefficient can then be expressed as the summation of Kirchhoff, cross and complementary scattering coefficient in the paper. The model predictions for upward and downward scatterings from rough surfaces are shown under different surface parameters; surface rms height, surface correlation length and surface rms slope. For studying the effect of backscattering enhancement we also show the relationship among the backscattering enhancement and multiple scattering strength. Finally the comparison of multiple scattering prediction and the measured data collected under controlled conditions from statistically rough surfaces was made over a wide frequency range and rms surface slope.

2. MODEL DEVELOPMENT

We first reformulate the integral equations for tangential surface fields on a dielectric interface. The purpose of this reformulation is to obtain the estimates of the tangential surface fields that are more general than the existing Kirchhoff or perturbation surface fields and reduce to known results under special conditions such as a perfectly conducting surface. The integral equation pairs given by Poggio and Miller [5] for the tangential surface electrical and magnetic fields in the dielectric medium are shown below.

$$\hat{n} \times \vec{E} = 2\hat{n} \times \vec{E}^i - \frac{2}{4\pi} \hat{n} \times \int \vec{E}'' ds'$$

and

$$\hat{n} \times \vec{H} = 2\hat{n} \times \vec{H}^i + \frac{2}{4\pi} \hat{n} \times \int \vec{H}'' ds' \quad (1)$$

In medium 2, we have

$$\begin{aligned} \hat{n}_t \times \vec{E}_t &= -\frac{2}{4\pi} \hat{n}_t \times \int \vec{E}_t'' ds' \\ \hat{n}_t \times \vec{H}_t &= \frac{2}{4\pi} \hat{n}_t \times \int \vec{H}_t'' ds' \end{aligned} \quad (2)$$

where

$$\begin{aligned} \vec{E}'' &= jk\eta(\hat{n}' \times \vec{H}')G - (\hat{n}' \times \vec{E}') \times \nabla'G - (\hat{n}' \cdot \vec{E}')\nabla'G \\ \vec{H}'' &= jk(\hat{n}' \times \vec{H}')G/\eta - (\hat{n}' \times \vec{H}') \times \nabla'G + (\hat{n}' \cdot \vec{H}')\nabla'G \end{aligned} \quad (3)$$

The fields in the lower medium can be written in terms of the fields in the upper medium by applying the boundary conditions on the continuity of the tangential fields.

The spectral representation for the Green's function and its gradient, i.e.,

$$G = \left(-\frac{1}{2\pi}\right) \int \frac{j}{q} \exp[ju(x-x') + jv(y-y') - jq|z-z'|] dudv \quad (4)$$

and

$$\nabla'G = \left(-\frac{1}{2\pi}\right) \int \frac{\vec{g}}{q} \exp[ju(x-x') + jv(y-y') - jq|z-z'|] dudv \quad (5)$$

where $q = \sqrt{k^2 - u^2 - v^2}$ and $\vec{g} = \hat{x}u + \hat{y}v \pm \hat{z}q$. z and z' are the random variables representing the surface height at different locations on surface. Without the absolute value term in the Green's function the ensemble average is the standard characteristic function for two, three and four random variables. When the phase term of the Green's function with an absolute value sign is included, the major impact is on the evaluation of the ensemble averages for finding the ensemble average scattered power.

2.1. Scattered Power and Coefficients

With the given Kirchhoff and complementary scattered field, the ensemble average scattered power is given by

$$\langle E_{qp}^s E_{qp}^{s*} \rangle = \langle E_{qp}^k E_{qp}^{k*} \rangle + 2\text{Re} \langle E_{qp}^c E_{qp}^{k*} \rangle = \langle E_{qp}^c E_{qp}^{c*} \rangle \quad (6)$$

where Re is the real part operator and $*$ is the symbol for complex conjugate. To obtain the incoherent power, we have to subtract the mean-squared power from the total power. That is,

$$\begin{aligned} \langle E_{qp}^s E_{qp}^{s*} \rangle - \langle E_{qp}^s \rangle \langle E_{qp}^s \rangle^* &= \langle E_{qp}^k E_{qp}^{k*} \rangle - \langle E_{qp}^k \rangle \langle E_{qp}^k \rangle^* \\ &+ \langle E_{qp}^c E_{qp}^{c*} \rangle - \langle E_{qp}^c \rangle \langle E_{qp}^c \rangle^* \\ &+ 2\text{Re} \left[\langle E_{qp}^c E_{qp}^{k*} \rangle - \langle E_{qp}^c \rangle \langle E_{qp}^k \rangle^* \right] \end{aligned} \quad (7)$$

The incoherent scattered power includes the Kirchhoff, cross and complementary scattered power. To carry out the average operation we must make an assumption about the type of surface height distribution. For the purpose of illustration we assume Gaussian height distribution here. The ensemble average scattered Kirchhoff, Cross and complementary terms are represented below respectively. The Kirchhoff ensemble average scattered power is

$$\begin{aligned} P_{qp}^k &= \langle E_{qp}^k E_{qp}^{k*} \rangle - \langle E_{qp}^k \rangle \langle E_{qp}^k \rangle^* \\ &= |CE_{of_{qp}}|^2 \left\{ \left\langle \iint \exp \left[j(\vec{k}_s - \vec{k}_i) \cdot (\vec{r} - \vec{r}') \right] dx' dy' dx dy \right\rangle \right. \\ &\quad \left. - \left| \left\langle \int \exp \left\{ j \left[(\vec{k}_s - \vec{k}_i) \cdot \vec{r} \right] \right\} dx dy \right| \right|^2 \right\} \end{aligned} \quad (8)$$

The cross scattered power is

$$\begin{aligned} P_{qp}^{kc} &= 2\text{Re} \left[\langle E_{qp}^c E_{qp}^{k*} \rangle - \langle E_{qp}^c \rangle \langle E_{qp}^k \rangle^* \right] \\ &= |(CE_o)/(2\pi)|^2 \text{Re} \left\{ \int (F_{qp} f_{qp}^*) \right. \\ &\quad \left. \iint \left\langle \exp \left[j\vec{k}_s \cdot (\vec{r} - \vec{r}'') + j\vec{k}_i \cdot (\vec{r}'' - \vec{r}') \right] \right. \right. \\ &\quad \left. \left. + ju(x - x') + jv(y - y') - jq|z - z'| \right] \right\rangle \\ &\quad - \left\langle \iint \exp \left[j(\vec{k}_s \cdot \vec{r}) - j(\vec{k}_i \cdot \vec{r}') \right] \right. \\ &\quad \left. + ju(x - x') + jv(y - y') - jq|z - z'| \right] \right\rangle \\ &\quad \left. \left\langle \int \exp \left\{ j \left[(\vec{k}_i - \vec{k}_s) \cdot \vec{r}'' \right] \right\} dx dy dx' dy' dx'' dy'' dudv \right\rangle \right\} \end{aligned} \quad (9)$$

and the complementary scattered power becomes

$$P_{qp}^c = \langle E_{qp}^c E_{qp}^{c*} \rangle - \langle E_{qp}^c \rangle \langle E_{qp}^c \rangle^*$$

$$\begin{aligned}
&= \left| (CE_o)/(8\pi^2) \right|^2 \operatorname{Re} \left\{ \int (F_{qp} F_{qp}^*) \right. \\
&\quad \left. \iiint \left\langle \exp \left[j\vec{k}_s \cdot (\vec{r} - \vec{r}'') + j\vec{k}_i \cdot (\vec{r}''' - \vec{r}') \right] \right. \right. \\
&\quad \left. \left. + ju(x - x') - ju'(x'' - x''') + jv(y - y') \right. \right. \\
&\quad \left. \left. - jv'(y'' - y''') - jq|z - z'| + jq'|z'' - z'''| \right] \right\rangle \\
&\quad dx dx' dx'' dx''' dy dy' dy'' dy''' dudv du' dv' \\
&\quad \left. - \left\langle \iiint F_{qp} \exp \left[j\vec{k}_s \cdot \vec{r} - j\vec{k}_i \cdot \vec{r}' + ju(x - x') \right. \right. \right. \\
&\quad \left. \left. + jv(y - y') - jq|z - z'| \right] dx dx' dy dy' dudv \right\rangle \right|^2 \quad (10)
\end{aligned}$$

The bistatic scattering coefficient is related to the ensemble average scattered power expression as

$$\sigma_{qp}^0 = (4\pi R^2 P_{qp}) / (E_0^2 A_0) \quad (11)$$

The incoherent ensemble average scattered power can be expressed as the summation of Kirchhoff, cross and complementary scattered power. Therefore the bistatic scattering coefficient can be summarized by Kirchhoff, cross and complementary scattered coefficient.

$$\sigma_{qp}^0 = \sigma_{qp}^k + \sigma_{qp}^{kc} + \sigma_{qp}^c \quad (12)$$

For evaluating the ensemble average we assume the rough surface is a Gaussian-distributed surface. The Fourier transform of the n th power of the Gaussian correlation function is

$$W^{(n)}(K) = \int_0^\infty \rho^n(\xi) J_o(K\xi) \xi d\xi = \frac{L^2}{2n} \exp \left[-\frac{(KL)^2}{4n} \right] \quad (13)$$

Therefore, the Fourier transform of the n th power of the Gaussian correlation function for numerical calculation can be expressed as

$$\begin{aligned}
&W^{(n)}(K_{sx} - k_x, k_{xy} - k_y) \\
&= \frac{L^2}{2n} \exp \left[-\frac{[(K_{sx} - k_x)^2 + (k_{sy} - k_y)^2] L^2}{4n} \right] \\
&= \frac{L^2}{2n} \exp \left[\frac{-(kL)^2 [(\sin \theta_s \cos \phi_s - \sin \theta \cos \phi)^2 + (\sin \theta_s \sin \phi_s - \sin \theta \sin \phi)^2]}{4n} \right] \quad (14)
\end{aligned}$$

Finally we split the scattering coefficient into two terms: a scattering coefficient for single scattering and the other one for multiple scattering. The single scattering terms are represented by terms with only one sum and do not involve the integration, while terms with more than one sum and the integration represent multiple scattering. The double sum term requires integration indicating the interaction among surface spectral components and hence represents multiple scattering.

The method of correction in single scattering is to multiply the scattering coefficient by the shadowing function. We summed up all terms including upward and downward single scattering for the single scattering coefficient. The single scattering coefficient with the Gaussian roughness spectrum and shadowing function for numerical calculation becomes

$$\sigma_{qp}^s = s(\theta_{in}) \cdot s(\theta) \cdot \frac{(kL)^2}{4} e^{-(k\sigma)^2(\cos^2\theta_s + \cos^2\theta)} \cdot \sum_{n=1}^{\infty} (k\sigma)^{2n} |I_{qp}|^2 \exp \left\{ -\frac{(kL)^2}{4n} [(\sin\theta_s \cos\phi_s - \sin\theta \cos\phi)^2 + (\sin\theta_s \sin\phi_s - \sin\theta \sin\phi)^2] \right\} \frac{1}{n \cdot n!} \tag{15}$$

where the item $|I_{qp}|^2$, the sum of three items, Kirchhoff, cross and complementary, is

$$\begin{aligned} |I_{qp}|^2 = & (\cos\theta_s + \cos\theta)^{2n} |f_{qp}|^2 \exp[-2(k\sigma)^2 \cos\theta_s \cos\theta \\ & + \frac{1}{2} \left\{ f_{qp}^* F_{qp}(-k_x, k_y) \left[\bar{c}_1^n(\bar{k}_z) \bar{r}_1(\bar{k}_z) + \bar{c}_1^n(-\bar{k}_z) \bar{r}_1(-\bar{k}_z) \right] \right. \\ & + f_{qp}^* F_{qp}(-k_{sx}, -k_{sy}) \left[\bar{c}_2^n(\bar{k}_{sz}) \bar{r}_1(\bar{k}_{sz}) + \bar{c}_2^n(-\bar{k}_{sz}) \bar{r}_1(-\bar{k}_{sz}) \right] \left. \right\} \\ & + \frac{1}{16} \left\{ |F_{qp}(-k_x, -k_y)|^2 \left[\bar{c}_3^n(\bar{k}_z, \bar{k}_z) \bar{r}_2(\bar{k}_z, \bar{k}_z) \right. \right. \\ & + \bar{c}_3^n(\bar{k}_z, -\bar{k}_z) \bar{r}_2(\bar{k}_z, -\bar{k}_z) + \bar{c}_3^n(-\bar{k}_z, \bar{k}_z) \bar{r}_2(-\bar{k}_z, \bar{k}_z) \\ & + \bar{c}_3^n(-\bar{k}_z, -\bar{k}_z) \bar{r}_2(-\bar{k}_z, -\bar{k}_z) \left. \right] + F_{qp}(-k_x, -k_y) F_{qp}^*(-k_{sx}, -k_{sy}) \\ & \cdot \left[\bar{c}_5^n(\bar{k}_z, \bar{k}_{sz}) \bar{r}_2(\bar{k}_z, \bar{k}_{sz}) + \bar{c}_5^n(\bar{k}_z, -\bar{k}_{sz}) \bar{r}_2(\bar{k}_z, -\bar{k}_{sz}) \right. \\ & + \bar{c}_5^n(-\bar{k}_z, \bar{k}_{sz}) \bar{r}_2(-\bar{k}_z, \bar{k}_{sz}) + \bar{c}_5^n(-\bar{k}_z, -\bar{k}_{sz}) \bar{r}_2(-\bar{k}_z, -\bar{k}_{sz}) \left. \right] \\ & + F_{qp}^*(-k_x, -k_y) F_{qp}(-k_{sx}, -k_{sy}) \left[\bar{c}_6^n(\bar{k}_{sz}, \bar{k}_z) \bar{r}_2(\bar{k}_{sz}, \bar{k}_z) \right. \\ & + \bar{c}_6^n(\bar{k}_{sz}, -\bar{k}_z) \bar{r}_2(\bar{k}_{sz}, -\bar{k}_z) + \bar{c}_6^n(-\bar{k}_{sz}, \bar{k}_z) \bar{r}_2(-\bar{k}_{sz}, \bar{k}_z) \\ & \left. + \bar{c}_6^n(-\bar{k}_{sz}, -\bar{k}_z) \bar{r}_2(-\bar{k}_{sz}, -\bar{k}_z) \right] |F_{qp}(-k_{sx}, -k_{sy})|^2 \end{aligned}$$

$$\cdot \left[\bar{c}_4^n(\bar{k}_{sz}, \bar{k}_{sz})\bar{r}_2(\bar{k}_{sz}, \bar{k}_{sz}) + \bar{c}_4^n(\bar{k}_{sz}, -\bar{k}_{sz})\bar{r}_2(\bar{k}_{sz}, -\bar{k}_{sz}) \right. \\ \left. + \bar{c}_4^n(-\bar{k}_{sz}, \bar{k}_{sz})\bar{r}_2(-\bar{k}_{sz}, \bar{k}_{sz}) + \bar{c}_4^n(-\bar{k}_{sz}, -\bar{k}_{sz})\bar{r}_2(-\bar{k}_{sz}, -\bar{k}_{sz}) \right] \Big\}$$

where

$$\begin{aligned} \bar{c}_1(\bar{q}) &= (\cos \theta_s - \bar{q}) \cos \theta_s + \cos \theta \\ \bar{c}_2(\bar{q}) &= (\cos \theta + \bar{q}) \cos \theta_s + \cos \theta \\ \bar{r}_1(\bar{q}) &= \exp[-(k\sigma)^2(\cos \theta \cos \theta_s + \bar{q}^2 - \cos \theta_s \cdot \bar{q} + \cos \theta \cdot \bar{q})] \\ \bar{c}_3(\bar{q}, \bar{q}') &= (\cos \theta_s - \bar{q})(\cos \theta_s - \bar{q}') \\ \bar{c}_4(\bar{q}, \bar{q}') &= (\cos \theta_s + \bar{q})(\cos \theta + \bar{q}') \\ \bar{c}_5(\bar{q}, \bar{q}') &= (\cos \theta_s - \bar{q})(\cos \theta + \bar{q}') \\ \bar{c}_6(\bar{q}, \bar{q}') &= (\cos \theta + \bar{q})(\cos \theta_s - \bar{q}') \\ \bar{r}_2(\bar{q}, \bar{q}') &= \exp \left\{ -(k\sigma)^2 [\bar{q}^2 + \bar{q}'^2 - \cos \theta_s(\bar{q} + \bar{q}') + \cos \theta(\bar{q} + \bar{q}')] \right\} \end{aligned}$$

$$\begin{aligned} \bar{k}_{sz} &= \cos \theta_s \\ \bar{k}_z &= \cos \theta \end{aligned}$$

2.2. Shadowing Functions

From Figure 2 the upward and downward multiple scattering coefficients need to be modified by the shadowing function. When the incident ray impinges on a randomly rough surface, a fraction, s , of the upward scattered signal leaves the surface interface permanently. The other part, $1 - s$, of the upward scattered signal is intercepted by the surface. This latter portion of the upward scattering coefficient becomes a source for multiple scattering. The downward scattered signal is intercepted by the surface and becomes the other kind of source for multiple scattering.

For multiple scattering two kinds of shadowing functions are needed to correct the multiple scattering coefficient: The first kind of the shadowing function is a function of the incident angle. The correction method is to multiply the scattering coefficient by the shadowing function directly. The second kind of shadowing function depends upon the incident angle of the rescattered field. Thus, the second correction method is to integrate the shadowing function. That means that the portion of the rescattered field intercepted by the surface along every direction needs to be modified by the shadowing function. The multiple scattered coefficient is modified by multiplying the first kind of the shadowing function $s(\theta_{in})$ and $s(\theta_s)$ outside the integrals. Inside the integrals the upward scattering coefficient is

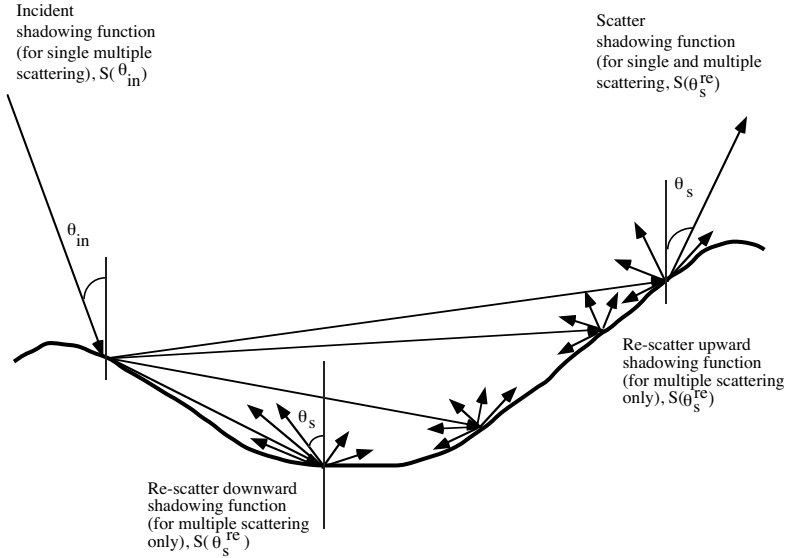


Figure 2. upward and downward scatterings.

modified by the second shadowing function, $1 - s(\theta)$, and the downward scattering coefficient is modified by the shadowing function $s(\theta)$. The total multiple-scatter scattering coefficient is the summation of upward and downward scattering coefficients.

For numerical calculation of ensemble average we assume the correlation coefficient $\rho(\xi, \varsigma)$ to be Gaussian given by

$$\rho(\xi, \varsigma) = \exp[-(\xi^2 + \varsigma^2)/l^2] \tag{16}$$

The properties of its partial derivative are

$$\rho_\xi(\xi, \varsigma) = \frac{-2\xi}{l^2} \cdot \exp[-(\xi^2 + \varsigma^2)/l^2] \tag{17}$$

and

$$\rho_\varsigma(\xi, \varsigma) = \frac{-2\varsigma}{l^2} \cdot \exp[-(\xi^2 + \varsigma^2)/l^2] \tag{18}$$

The values of the second partial derivative about the origin are therefore

$$\rho_{\xi\xi}(0) = \frac{-2}{l^2} \tag{19}$$

$$\rho_{\varsigma\varsigma}(0) = \frac{-2}{l^2} \tag{20}$$

and

$$\rho_{\xi\xi}(0) = 0 \quad (21)$$

2.3. Scattering Coefficients with Shadowing Functions

The multiple scattering coefficient with shadowing function inside and outside the integral for numerical calculation is therefore expressed as

$$\sigma_{qp}^m(L)_{(total)} = \sigma_{qp}^m(L)_{(upward)} + \sigma_{qp}^m(L)_{(downward)} \quad (22)$$

where

$$\begin{aligned} \sigma_{qp}^m(L)_{(upward)} = & s(\theta_{in})s(\theta) \frac{(kL)^4}{16\pi(k\sigma)^4} \left\{ \frac{1}{2} \int \text{Re} \left[f_{qp}^* F_{qp}(u, v) \right] \cdot c_1(\bar{q})c_2(\bar{q}) \right. \\ & + \frac{1}{16} \int |F_{qp}(u, v)|^2 [c_3(\bar{q}, \bar{q}')c_4(\bar{q}, \bar{q}') + c_3(\bar{q}, -\bar{q}')c_4(\bar{q}, -\bar{q}')] \\ & + \frac{1}{16} \int F_{qp}(u, v)F_{qp}^*(-u - k_{sx} - k_x, -v - k_{sy} - k_y) \\ & \left[\exp \left[-(k\sigma)^2(\cos \theta_s - \cos \theta - \bar{q} - \bar{q}')^2 \right] c_5(\bar{q}, \bar{q}')c_6(\bar{q}, \bar{q}') + \right. \\ & \left. \exp \left[-(k\sigma)^2(\cos \theta_s - \cos \theta - \bar{q} + \bar{q}')^2 \right] c_5(\bar{q}, -\bar{q}')c_6(\bar{q}, -\bar{q}') \right] \\ & + \left(\frac{1}{4} \right) \frac{(kL)^2}{8\pi} \int F_{qp}(u, v) \left\{ \int F_{qp}^*(u', v') \right. \\ & \left[\sum_{n=1}^{\infty} \frac{[(k\sigma)^2(\cos \theta_s - \cos \theta - \bar{q} - \bar{q}')^2]^n \bar{W}^{(n)}(\dots)}{n!} \right. \\ & \cdot c_5(\bar{q}, \bar{q}')c_6(\bar{q}, \bar{q}') \exp[-(k\sigma)^2(\cos \theta_s - \cos \theta - \bar{q} - \bar{q}')^2] \\ & + \sum_{n=1}^{\infty} \frac{[(k\sigma)^2(\cos \theta_s - \cos \theta - \bar{q} + \bar{q}')^2]^n \bar{W}^{(n)}(\dots)}{n!} \\ & \cdot c_5(\bar{q}, -\bar{q}')c_6(\bar{q}, -\bar{q}') \exp[-(k\sigma)^2(\cos \theta_s - \cos \theta - \bar{q} + \bar{q}')^2] \left. \right] \\ & \left. \left. [1 - s(\theta)]x_2 dx_2 d\delta \right\} \right\} [1 - s(\theta)]x dx d\delta \end{aligned}$$

and

$$\begin{aligned} \sigma_{qp}^m(L)_{(downward)} = & s(\theta_{in})s(\theta) \frac{(kL)^4}{16\pi(k\sigma)^4} \left\{ \frac{1}{2} \int \text{Re} \left[f_{qp}^* F_{qp}(u, v) \right] \cdot c_1(-\bar{q})c_2(-\bar{q}) \right. \end{aligned}$$

$$\begin{aligned}
 & + \frac{1}{16} \int |F_{qp}(u, v)|^2 [c_3(-\bar{q}, \bar{q}')c_4(-\bar{q}, \bar{q}') + c_3(-\bar{q}, -\bar{q}')c_4(-\bar{q}, -\bar{q}')] \\
 & + \frac{1}{16} \int F_{qp}(u, v)F_{qp}^*(-u - k_{sx} - k_x, -v - k_{sy} - k_y) \\
 & \left[\exp \left[-(k\sigma)^2 (\cos \theta_s - \cos \theta + \bar{q} - \bar{q}')^2 \right] c_5(-\bar{q}, \bar{q}')c_6(-\bar{q}, \bar{q}') + \right. \\
 & \left. \exp \left[-(k\sigma)^2 (\cos \theta_s - \cos \theta + \bar{q} + \bar{q}')^2 \right] c_5(-\bar{q}, -\bar{q}')c_6(-\bar{q}, -\bar{q}') \right] \\
 & + \left(\frac{1}{4} \right) \frac{(kL)^2}{8\pi} \int F_{qp}(u, v) \left\{ \int F_{qp}^*(u', v') \right. \\
 & \left[\sum_{n=1}^{\infty} \frac{[(k\sigma)^2 (\cos \theta_s - \cos \theta + \bar{q} - \bar{q}')^2]^n \bar{W}^{(n)}(\dots)}{n!} \right. \\
 & \cdot c_5(-\bar{q}, \bar{q}')c_6(-\bar{q}, -\bar{q}') \exp[-(k\sigma)^2 (\cos \theta_s - \cos \theta + \bar{q} - \bar{q}')^2] \\
 & + \sum_{n=1}^{\infty} \frac{[(k\sigma)^2 (\cos \theta_s - \cos \theta + \bar{q} + \bar{q}')^2]^n \bar{W}^{(n)}(\dots)}{n!} \\
 & \cdot c_5(-\bar{q}, \bar{q}')c_6(-\bar{q}, \bar{q}') \exp[-(k\sigma)^2 (\cos \theta_s - \cos \theta + \bar{q} + \bar{q}')^2] \left. \right\} \\
 & \left. s(\theta) x_2 dx_2 d\delta \right\} s(\theta) x dx d\delta
 \end{aligned}$$

where

$$\begin{aligned}
 c_1(\bar{q}) &= \frac{\exp \left[-\frac{(kL)^2 \cdot SXY'}{4(k\sigma)^2 (\cos \theta_s - \bar{q})(\cos \theta_s + \cos \theta)} \right]}{(\cos \theta_s - \bar{q})(\cos \theta_s + \cos \theta)} \\
 c_2(\bar{q}) &= \frac{\exp \left[-\frac{(kL)^2 \cdot XY'}{4(k\sigma)^2 (\cos \theta_s + \bar{q})(\cos \theta_s + \cos \theta)} \right]}{(\cos \theta_s + \bar{q})(\cos \theta_s + \cos \theta)} \\
 c_3(\bar{q}, \bar{q}') &= \frac{\exp \left[-\frac{(kL)^2 \cdot SXY'}{4(k\sigma)^2 (\cos \theta_s - \bar{q})(\cos \theta_s - \bar{q}')} \right]}{(\cos \theta_s - \bar{q}')(\cos \theta_s - \bar{q}')} \\
 c_4(\bar{q}, \bar{q}') &= \frac{\exp \left[-\frac{(kL)^2 \cdot XY'}{4(k\sigma)^2 (\cos \theta + \bar{q})(\cos \theta + \bar{q}')} \right]}{(\cos \theta + \bar{q}')(\cos \theta + \bar{q}')}
 \end{aligned}$$

$$\begin{aligned}
c_5(\bar{q}, \bar{q}') &= \frac{\exp \left[-\frac{(kL)^2 \cdot SXY'}{4(k\sigma)^2(\cos \theta_s - \bar{q})(\cos \theta + \bar{q}')} \right]}{(\cos \theta_s - \bar{q}')(\cos \theta + \bar{q}')} \\
c_6(\bar{q}, \bar{q}') &= \frac{\exp \left[-\frac{(kL)^2 \cdot XY'}{4(k\sigma)^2(\cos \theta + \bar{q})(\cos \theta - \bar{q}')} \right]}{(\cos \theta + \bar{q}')(\cos \theta_s - \bar{q}')} \\
SXY' &= (\sin \theta_s \cos \phi_s + x \cos \delta)^2 + (\sin \theta_s \sin \phi_s + x \sin \delta)^2 \\
XY' &= (\sin \theta \cos \phi + x \cos \delta)^2 + (\sin \theta \sin \phi + x \sin \delta)^2 \quad (23)
\end{aligned}$$

and

$$\begin{aligned}
\overline{W}^{(n)}(\dots) &= \\
&\frac{1}{2n} \exp \left[-\frac{(kL)^2(x \cos \delta + x_2 \cos \delta_2 + \sin \theta_s \cos \phi_s + \sin \theta \cos \phi)^2}{4n} \right] \\
&\cdot \exp \left[-\frac{(kL)^2(x \sin \delta + x_2 \sin \delta_2 + \sin \theta_s \sin \phi_s + \sin \theta \sin \phi)^2}{4n} \right] \\
&\equiv W^{(n)}(\dots)/L^2 \quad (24)
\end{aligned}$$

The last terms with four integrals in the multiple scattering coefficient is small. If the term $(k_{sz} - k_z \pm q \pm q')$ is small, the term of $(k_{sz} - k_z \pm q \pm q')^2$ has a relatively small value compare to the other terms in multiple scattering coefficient. If $(k_{sz} - k_z \pm q \pm q')$ term is large, the factor, $\exp[-\sigma^2(k_{sz} - k_z \pm q \pm q')^2]$, makes the four-integral term small comparing to the other terms in the multiple scattering coefficient. Thus, the four-integral term takes a long time in calculation; it can be ignored and has very little effect on the final result.

3. SHADOWING FUNCTIONS

The explicit focus of the shadowing functions for the incident and scattered waves are (1) In single scattering the shadowing function for the incident waves depends upon the cotangent of the incident angle. The incident shadowing function $s(\theta_{in}, \sigma_s)$ is

$$s(\theta_{in}, \sigma_s) = \left[1 - \frac{1}{2} \operatorname{erfc} \left(\frac{\cot \theta_{in}}{\sigma_s \sqrt{2}} \right) \right] [1 + f(\theta_{in}, \sigma_s)]^{-1} \quad (25)$$

where

$$f(\theta_{in}, \sigma_s) = \frac{1}{2} \left\{ \sqrt{\frac{2}{\pi}} \frac{\sigma_s \sqrt{2}}{\cot \theta_{in}} \exp \left(-\frac{\cot^2 \theta_{in}}{2\sigma_s^2} \right) - \operatorname{erfc} \left(\frac{\cot \theta_{in}}{\sigma_s \sqrt{2}} \right) \right\} \quad (26)$$

(2) In single scattering the shadowing function for the scatter waves depends upon the cotangent of the scatter angle, $\cot \theta_s$. The scatter shadowing function $s(\theta_s, \sigma_s)$ is

$$s(\theta_s, \sigma_s) = \left[1 - \frac{1}{2} \operatorname{erfc} \left(\frac{\cot \theta_s}{\sigma_s \sqrt{2}} \right) \right] [1 + f(\theta_s, \sigma_s)]^{-1} \quad (27)$$

where

$$f(\theta_s, \sigma_s) = \frac{1}{2} \left\{ \sqrt{\frac{2}{\pi}} \frac{\sigma_s \sqrt{2}}{\cot \theta_s} \exp \left(-\frac{\cot^2 \theta_s}{2\sigma_s^2} \right) - \operatorname{erfc} \left(\frac{\cot \theta_s}{\sigma_s \sqrt{2}} \right) \right\} \quad (28)$$

3.1. Shadowing Functions under the Integral Sign

The rescattered shadowing function $s(\theta, \sigma_s)$ inside the integration is expressed as

$$s(\theta, \sigma_s) = s(x, \sigma_s) = \left[1 - \frac{1}{2} \operatorname{erfc} \left(\frac{\cot \theta}{\sigma_s \sqrt{2}} \right) \right] [1 + f(\theta, \sigma_s)]^{-1} \quad (29)$$

where

$$f(\theta, \sigma_s) = \frac{1}{2} \left\{ \sqrt{\frac{2}{\pi}} \frac{\sigma_s \sqrt{2}}{\cot \theta} \exp \left(-\frac{\cot^2 \theta}{2\sigma_s^2} \right) - \operatorname{erfc} \left(\frac{\cot \theta}{\sigma_s \sqrt{2}} \right) \right\} \quad (30)$$

In multiple scattering the shadowing function depends upon the cotangent of the incident angle θ^{re} of the rescattered field, i.e.,

$$\cot \theta^{re} = \frac{\sqrt{k^2 - u^2 - v^2}}{\sqrt{u^2 + v^2}} = \sqrt{\frac{1}{x^2} - 1} \quad (31)$$

where

$$u = r \cos \delta \quad (32)$$

$$v = r \sin \delta \quad (33)$$

and x is the normalized value of r , i.e.

$$x = \frac{r}{k} \quad (34)$$

The different u and v value of the shadowing function in multiple scattering represents different scattering directions.

4. MODEL PREDICTION

To assess the conditions under which multiple scattering becomes important, we show the effect of surface parameters (surface standard deviation, surface correlation length) and operation frequency. In general the single scattering is the major contribution to the like-polarized scattering, but the multiple scattering is the only contribution to the cross-polarized scattering. The model predictions shown in this section to predict the depolarized bistatic scattering behavior is based upon the integral equation pairs.

4.1. Contribution Comparisons of Single and Multiple Scattering

First we show the comparisons of depolarized single and multiple scattering from two rough surfaces in Figures 3 and 4. Two rough surface have the same surface parameters; normalized surface height of 4.4 and normalized surface correlation length of 13.2, but their dielectric constant are different. One rough surface has water-soaked form bricks material with an estimated relative dielectric constant of 62

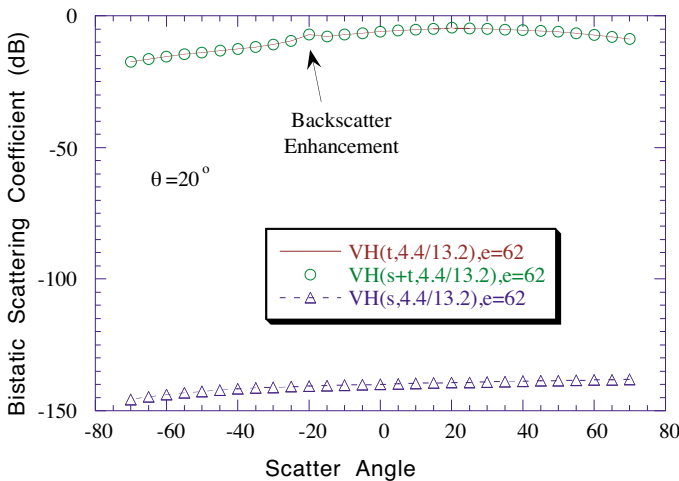


Figure 3. Comparisons of single(s), total(t) multiple and the summation of single and multiple($s + t$) scattering coefficients from a rough surface with normalized surface height of 4.4, normalized surface correlation length of 13.2 and dielectric constant of 62. The incident angle is chosen to be 20 degree.

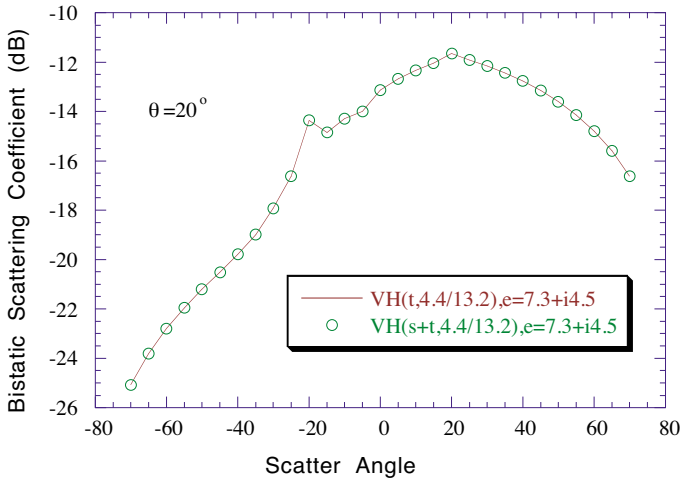


Figure 4. Comparisons of single(s), total(t) multiple and the summation of single and multiple($s + t$) scattering coefficients from a rough surface with normalized surface height of 4.4, normalized surface correlation length of 13.2 and complex dielectric constant of $7.3 + i4.5$.

($\epsilon_r = 62$), but the other one has the complex relative dielectric constant of $7.3 + i4.5$ ($\epsilon_r = 7.3 + j4.5$). In Figures 3 and 4 the depolarized bistatic scattering are generally dominated by multiple scattering along the plane of incidence, because its single scattering term is negligible in this specular plane. The effect of backscattering enhancement is normally accompanied by a large depolarized component. The enhancement peak usually has a small angular width, typically 2 to 3 degrees.

4.2. Upward and Downward Multiple Scattering

For depolarized bistatic scattering the depolarized backscatter enhancement comes mainly from the constructive interference of multiple scattering from Figures 3 and 4. In this section we compare the contributions of upward and downward scattering strength to the backscatter enhancement from rough surfaces along the plane of incidence. In Figures 5 through 8 we show the comparisons of upward, downward and total multiple scattering coefficients from a perfectly conducting rough surface and two dielectric rough surface with normalized surface height of 4.4. Two normalized surface correlation lengths are 13.2 and 17.6 respectively. Two relative dielectric constants are 62 and $7.3 + i4.5$. In Figures 5 through 8 the scatter pattern of backscatter enhancement comes from the contribution of both upward

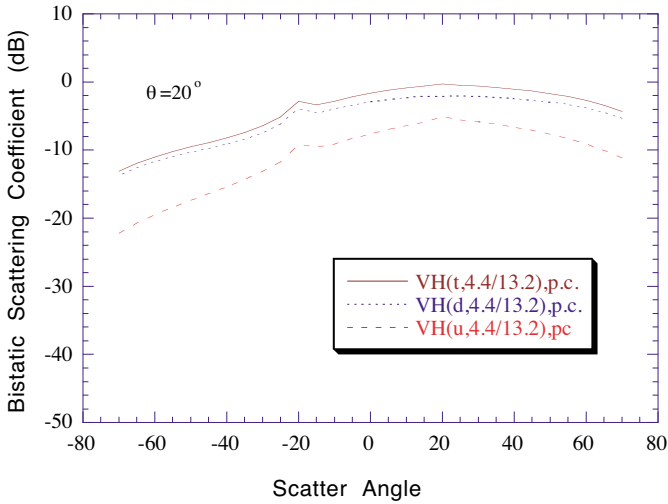


Figure 5. Comparisons of upward(u), downward(d) and total(t) multiple scattering coefficients from perfectly conducting rough surfaces normalized surface height of 4.4 and normalized surface correlation length of 17.6.

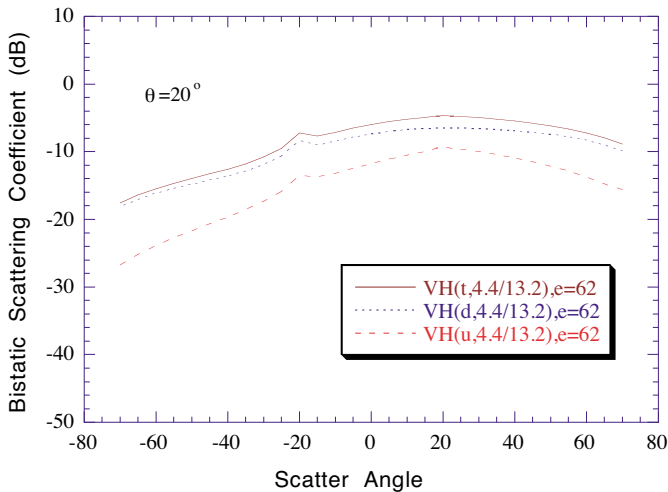


Figure 6. Comparisons of upward(u), downward(d) and total(t) multiple scattering coefficients from a dielectric rough surface with normalized surface height of 4.4, normalized surface correlation length of 17.6 and dielectric constant of 62.

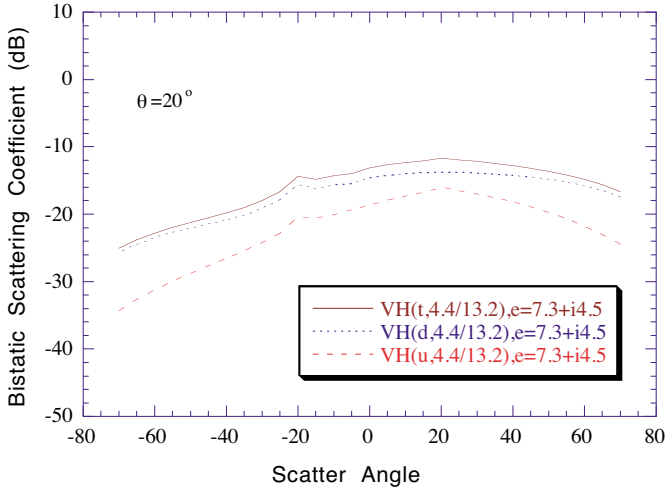


Figure 7. Comparisons of upward(u), downward(d) and total(t) multiple scattering coefficients from a dielectric rough surface with normalized surface height of 4.4, normalized surface correlation length of 13.2 and complex dielectric constant of $7.3 + i4.5$.

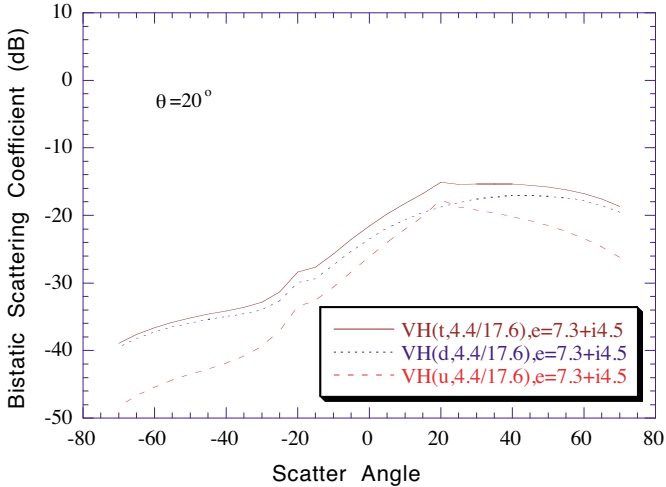


Figure 8. Comparisons of upward(u), downward(d) and total(t) multiple scattering coefficients from a dielectric rough surface with normalized surface height of 4.4 with the wavenumber k ($k\sigma = 4.4$), normalized surface correlation length of 17.6 and complex dielectric constant of $7.3 + i4.5$.

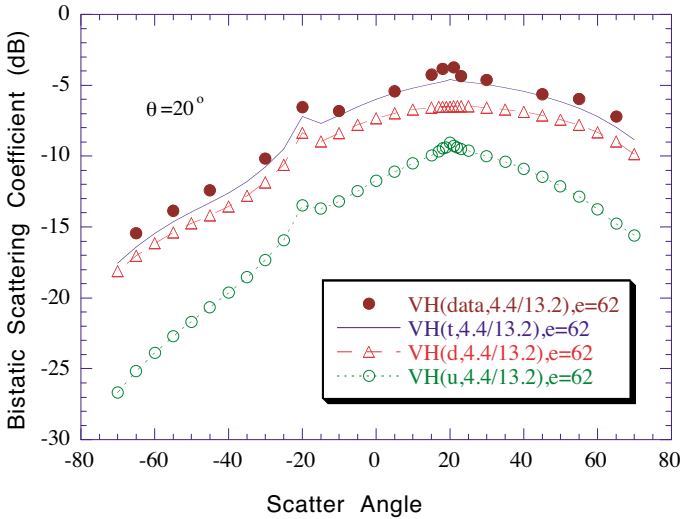


Figure 9. Comparison of model prediction of depolarized multiple scattering with the measured data from rough surface with normalized surface rms height of 4.4 with the wavenumber k ($k\sigma = 4.4$), normalized surface correlation length of 13.2 with the wavenumber k ($k\sigma = 4.4$) and dielectric surface of 62.

and downward scattering and the strength of downward scattering is always larger than that of upward scattering. The scatter energy may transfer among in the upward and downward directions. The amount of energy transfer depends upon the surface roughness; surface rms height, surface correlation length and rms surface slope. The strength of upward scattering in the forward scattering direction is always larger than that in the backward direction, but the strength of downward scattering in the forward scattering direction is always less than that in the backward direction. This phenomenon happens due to the energy transfer and surface parameters. With the comparisons of bistatic scattering pattern shown in Figures 7 and 8, the upward scattering strength increases and downward scattering strength decreases for rough surface with smaller rms surface slope in Figure 8. Further increase in surface rms slope causes the specular peak to disappear and a significant backscattering enhanced peak to appear.

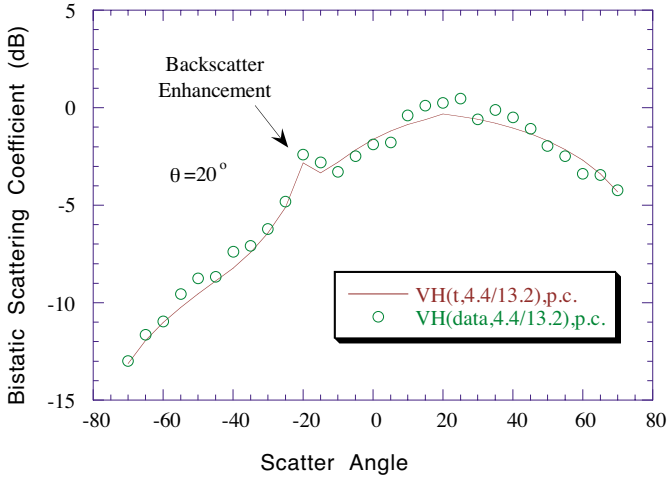


Figure 10. Comparison of model prediction of depolarized multiple scattering with the measured data from a perfectly conducting rough surface with normalized surface rms height of 4.4 with the wavenumber k ($k\sigma = 4.4$) and normalized surface correlation length of 13.2. The incident angle is chosen to be 20 degree.

5. COMPARISONS WITH MEASUREMENTS

To evaluate the validity of model prediction for the depolarized multiple scattering for very rough surfaces we compare the level and trend of depolarized scattering coefficient of model prediction with the measured data. The measurements shown were acquired from three rough surfaces with different dielectric constant. The normalized surface correlation length is 13.2 with the wavenumber k ($kL = 13.2$) and surface standard deviation is 4.4 with the wavenumber k ($k\sigma = 4.4$). The incident angle is chosen to be 20 degrees. In Figures 9 and 10 the specular peak and the backscattering peak decreases for the surface dielectric constant decreases due to scatter energy transmitting into the second medium. Figure 10 shows the comparisons of the model prediction of bistatic scattering behavior with the measurements at an incident angle of 20 degrees from a perfectly conducting rough surface in the incidence plane. The difference among two models is less than a dB. For further evaluating the model developed in this paper we also compare the integral equation model's prediction with the measured data from rough surface with dielectric constant of 62 and find the difference is still less than a dB.

APPENDIX A.

Using the transformation of coordinate system, two terms of ensemble average with multiple random variables and the absolute phase terms are listed below:

$$\begin{aligned}
& \langle \exp[jk_{sz}(z - z'') - jk_z(z'' - z')] - jq|z - z'| \rangle \\
= & \frac{1}{2} \exp \left\{ \sigma^2 [(k_{sz} - q)(k_{sz} + k_z)\rho_2(\xi, \varsigma) + (k_z + q)(k_{sz} + k_z)\rho_3(\xi', \varsigma')] \right\} \\
& \cdot \exp \left\{ - \left[k_{sz}^2 + k_z^2 + k_{sz}k_z + q^2 - qk_{sz} + qk_z + (k_{sz}k_z - q^2 + qk_{sz} - qk_z) \right. \right. \\
& \left. \left. \rho_1(\xi - \xi', \varsigma - \varsigma') \right] \sigma^2 \right\} \\
& + \frac{1}{2} \exp \left\{ \sigma^2 [(k_{sz} + q)(k_{sz} + k_z)\rho_2(\xi, \varsigma) + (k_z - q)(k_{sz} + k_z)\rho_3(\xi', \varsigma')] \right\} \\
& \cdot \exp \left\{ - \left[k_{sz}^2 + k_z^2 + k_{sz}k_z + q^2 + qk_{sz} - qk_z + (k_{sz}k_z - q^2 - qk_{sz} + qk_z) \right. \right. \\
& \left. \left. \rho_1(\xi - \xi', \varsigma - \varsigma') \right] \sigma^2 \right\} \tag{A1}
\end{aligned}$$

$$\begin{aligned}
& \langle \exp[jk_{sz}z + jk_zz'] - jq|z - z'| \rangle \\
= & \frac{1}{2} \exp \left\{ - \left[k_{sz}^2 + k_z^2 + 2(q^2 - qk_{sz} + qk_z) \right. \right. \\
& \left. \left. + 2(k_{sz}k_z - q^2 + qk_{sz} - qk_z) \rho_1(\xi - \xi', \varsigma - \varsigma') \right] (\sigma^2/2) \right\} \\
& + \frac{1}{2} \exp \left\{ - \left[k_{sz}^2 + k_z^2 + 2(q^2 + qk_{sz} - qk_z) \right. \right. \\
& \left. \left. + 2(k_{sz}k_z - q^2 - qk_{sz} + qk_z) \rho_1(\xi - \xi', \varsigma - \varsigma') \right] (\sigma^2/2) \right\} \tag{A2}
\end{aligned}$$

REFERENCES

1. Ailes-Sengers, L., A. Ishimaru, and Y. Kuga, "Analytical and experimental studies of electromagnetic waves scattered by two-dimensional, dielectric very rough surfaces," *International Geoscience and Remote Sensing Symposium*, Vol. 2, 1349-1351, 1995.
2. Johnson, J. T., R. T Shin, L. Tsang, C. H. Chan, A. Ishimaru, and Y. Koga, "Backscattering enhancement of electromagnetic waves from two-dimensional perfectly conducting random rough surfaces: A comparison of Monte Carlo simulations with experimental data," *IEEE Transactions on Antennas and Propagations*, Vol. 44, No. 5, 748-755, 1996.
3. Kuga, Y. and H. Zhao, "Experimental studies on the phase

- distribution of two copolarized signals scattered from two-dimensional rough surfaces," *IEEE Transactions on Geoscience and Remote Sensing*, Vol. 34, No. 2, 601–603, 1996.
4. Ocla, H. E. and M. Tateiba, "Backscattering enhancement in radar cross-section for concave-convex targets in random media," *IEEE 2000 International Geoscience and Remote Sensing Symposium*, Vol. 4, 1720–1722, 2000.
 5. Hsieh, C.-Y., "Dependence of backscattering enhancement from randomly very rough surfaces," *IEEE 1999 International Geoscience and Remote Sensing Symposium*, Vol. 4, 2197–2199, 1999.
 6. Hsieh, C.-Y. and A. K. Fung, "Application of an extended IEM to multiple surface scattering and backscatter enhancement," *IEEE International Geoscience and Remote Sensing*, Vol. 2, 702–704, 1997.
 7. Poggio, A. J. and E. K. Miller, *Integral Equation Solution of Three Dimensional Scattering Problems, Computer Techniques for Electromagnetics*, Chapter 4, Pergamon, New York, 1973.
 8. Smith, R. G., "Geometrical shadowing of randomly rough surfaces," *IEEE Trans. Antenna Propagation*, Vol. AP-15, 668–671, 1967.

Chin-Yuan Hsieh was born in Kaohsiung, Taiwan, R.O.C.. He received the B.S. degree from the National Taiwan Ocean University, the M.S. degree from the University of Missouri at Columbia, and the Ph.D. degree from The University of Texas at Arlington respectively, all in Electrical Engineering. In 1980, he passed the highest civil examination of electrical engineering in Taiwan. From 1982 to 1986, he was the director of the Department of Quality Control at the Bureau of Quality Inspection, Ministry of Economics in Taiwan, where he supervised studies in electromagnetic interference. From 1986 to 1988, he was the Director of the Microwave Communication Department, Taipei City Broadcasting Station where he supervised the design, development, and the construction of the microwave communication and links. In 1990, he became a faculty member at National Kaohsiung Marine University, where he is currently a full professor in the department of Electronics Communications Engineering. He is also an Engineering Dean in the college of marine Engineering and also the dean of the Night School & Extension Education at National Kaohsiung Marine University. He is author of *Electromagnetics*, Chuan-Hwa Books Co., Taipei, Taiwan, 1996

and author of *Communications System*, Chuan-Hwa Books Co., Taipei, Taiwan, 1996. He received the 1999 distinguished research award from National Science Foundation, Taiwan, R.O.C. He is also rewarded a “Marquis Who’s Who in the World, The chronicle of Human Achievement” in 2003 and 2004. His main research interests concern the model development of bistatic and multistatic polarimetric scattering, remote sensing, radar imaging, subsurface sensing, and numerical techniques in electromagnetics. Dr. Hsieh is a member of Institute of Electrical and Electronic Engineers (IEEE), Tau Beta Pi, and Alpha Beta Delta.

Adrian K. Fung has been conducting funded research sponsored by the National Science Foundation, U.S. Army Research Office, Navy, DARPA, NASA and other U.S. government agencies. He was with the Electrical Engineering Department of the University of Kansas from 1965 to 1984. He has been a consultant to the U.S. Army, U.S. Navy, NASA, the European Space Agency, and the International Advisory Panel in Washington, D.C. He is the author of *Microwave Scattering Models and Their Applications*, 1994, and a co-author of a three volume series on Microwave Remote Sensing. He is the recipient of an award from the European Chapter of the IEEE Geoscience and Remote Sensing Society for his contribution to microwave scattering theory in 1984, and he also received the Distinguished Achievement Award from IEEE Geoscience and Remote Sensing Society in 1989. Dr. Fung is a Fellow of the Institute of Electrical and Electronic Engineers.